BIOCHEMISTRY
including biophysical chemistry & molecular biology

Article

pubs.acs.org/biochemistry

Paramagnetic Nuclear Magnetic Resonance Relaxation and Molecular Mechanics Studies of the Chloroperoxidase−Indole Complex: Insights into the Mechanism of Chloroperoxidase-Catalyzed Regioselective Oxidation of Indole

Rui Zhang, Qinghao He, David Chatfield, and Xiaotang Wang*

Department of Chemistry and Biochemistry, Florida International University, Miami, Florida 33199, United States

Supporting Information

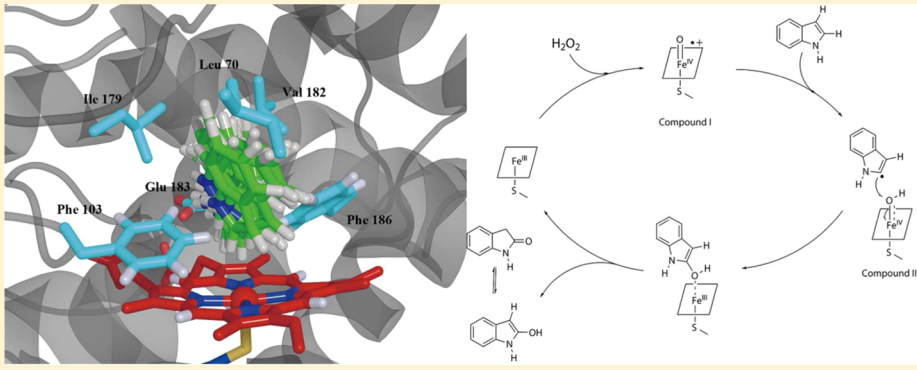

ABSTRACT: To unravel the mechanism of chloroperoxidase (CPO)-catalyzed regioselective oxidation of indole, we studied the structure of the CPO−indole complex using nuclear magnetic resonance (NMR) relaxation measurements and computational techniques. The dissociation constant (K_D) of the CPO−indole complex was calculated to be approximately 21 mM. The distances (r) between protons of indole and the heme iron calculated via NMR relaxation measurements and molecular docking revealed that the pyrrole ring of indole is oriented toward the heme with its 2-H pointing directly at the heme iron. Both K_D and r values are independent of pH in the range of 3.0−6.5. The stability and structure of the CPO−indole complex are also independent of the concentration of chloride or iodide ion. Molecular docking suggests the formation of a hydrogen bond between the NH group of indole and the carboxyl O of Glu 183 in the binding of indole to CPO. Simulated annealing of the CPO−indole complex using r values from NMR experiments as distance restraints reveals that the van der Waals interactions were much stronger than the Coulomb interactions in the binding of indole to CPO, indicating that the association of indole with CPO is primarily governed by hydrophobic rather than electrostatic interactions. This work provides the first experimental and theoretical evidence of the long-sought mechanism that leads to the "unexpected" regioselectivity of the CPO-catalyzed oxidation of indole. The structure of the CPO−indole complex will serve as a lighthouse in guiding the design of CPO mutants with tailor-made activities for biotechnological applications.

Chloroperoxidase (CPO), a heme-thiolate protein secreted by the marine fungus *Caldariomyces fumago*,[1] is a versatile enzyme[2] capable of catalyzing a broad spectrum of chemical reactions, including halogenation,[3] dehalogenation,[4] N-demethylation,[5] dismutation,[1] epoxidation,[6] and oxidation.[7−11] Therefore, CPO has been the subject of numerous biotechnological investigations because of its potential applications in synthetic chemistry as well as the pharmaceutical industry.[12−15] Most interestingly, CPO-catalyzed oxidation and epoxidation reactions proceed with high regio- and enantioselectivity.[6,8,16] Tremendous efforts have been made during the past few decades to understand the mechanism of CPO's regio- and enantioselectivity.[17−19] Most such studies are focused on the structures of CPO−substrate complexes. The structural feature of CPO−substrate complexes will shed light on the structure−function relationships of heme proteins in general and the structural basis of the diverse catalytic activity, strict substrate specificity, and high regio- and enatioselectivity displayed by CPO in particular. The definitive structure of CPO−substrate complexes will also provide pivotal information regarding the topology of the heme active center of CPO, the residues involved in the catalytic cycle, the location and/or orientation of substrate binding, and the mechanisms of CPO-catalyzed reactions. Such information will serve as a lighthouse for designing more efficient CPO mutants that target specific substrates and produce desired products that are difficult to

Received: February 26, 2013
Revised: May 1, 2013
Published: May 1, 2013

   dx.doi.org/10.1021/bi4002437 | *Biochemistry* 2013, 52, 3688−3701

obtain under mild conditions.[20] Unfortunately, the structural information about CPO−substrate complexes remains scarce despite the great efforts made with the application of the most powerful available techniques, including X-ray crystallography and nuclear magnetic resonance (NMR) spectroscopy.

X-ray crystal crystallography is one of the most powerful techniques for elucidating the three-dimensional structure of enzymes and their complexes with substrates. The crystal structure of CPO has demonstrated the presence of a substrate-binding site with an opening above the heme that allows organic substrates to approach the oxoferryl oxygen of CPO compound I.[2] It is generally expected that substrate binding would result in noticeable structural changes to the protein. Surprisingly, the structures of CPO−ligand complexes are indistinguishable from that of the ligand-free protein.[21] On the other hand, the crystal structure of CPO complexed with its natural substrate, 1,3-cyclopentanedione (CPDO) (PDB entry 2CIX), revealed another surprising picture in which the active methylene group of CPDO is not oriented toward the heme iron.[22] This is in good agreement with the results reported from an NMR relaxation study of the CPO−CPDO complex in solution.[23] To date, 2CIX is the only crystal structure of CPO complexed with a substrate. The limited crystal structural data on CPO−substrate complexes are mainly attributed to the difficulty of diffusing organic substrates into CPO crystals.[22]

Nuclear magnetic resonance (NMR) spectroscopy is an alternative technique to X-ray crystallography for probing the structural information of proteins and their complexes with substrates in solution. In particular, in heme proteins, the enhanced nuclear relaxation induced by the paramagnetism of the heme[24,25] was often used to establish the structure and stability of the enzyme−substrate complex.[24,26,27] NMR relaxation studies have been successfully used in determining the structural features of CPO complexed with various substrates, including phenols,[28] sulfides,[29] and the natural chlorination substrate, CPDO.[23]

Molecular mechanics studies have become an important complement to NMR and X-ray experiments in exploring heme proteins and their interactions with substrates at the atomic level.[30,31] The NMR-determined distances between the substrate and the heme iron can be used as restraints in simulation studies utilizing a simulated annealing protocol.[32,33] This protocol has been successfully applied to studies of binding of substrates to several other hemoproteins.[34,35] This success has prompted us to investigate the mechanisms of CPO-catalyzed regioselective oxidation of indole using both NMR and computational techniques.

The CPO-catalyzed oxidation of indole to oxindole was first reported in 1979.[36] van Deurzen et al. further reported that the oxidation of substituted indoles yields the corresponding oxindoles and the reactivity of the substituted indoles depends on the nature and position of their substituent.[37] However, to the best of our knowledge, the structural basis for CPO-catalyzed unusual regioselective oxidation of indole remains undefined. On the basis of the structure of indole, the oxidation would be expected to occur at position 3 of indole, which possesses the highest electron density and is thus most susceptible to attack by oxidizing agents and by other electrophilic reagents.[36] It is obvious to suspect the indolic NH group as a structural feature controlling the position of oxidation, even though indole is an extremely weak base. However, the presence of a hydrogen bond between the indole NH group and an unknown group at the CPO active site has proven to be insufficient to explain the regiospecificity of indole oxidation.[36] Therefore, a detailed structural characterization of the CPO−indole complex would offer greater insight into the mechanisms of CPO-catalyzed oxidations and solve the long-lasting puzzle of the unusual product from indole oxidation.

The aims of this work are to reveal the orientation of indole binding at the active site of CPO, to identify the residues involved in the formation of the CPO−indole complex, and to elucidate the mechanism of CPO-catalyzed regioselective oxidation of indole. The interaction of indole with CPO was probed using longitudinal NMR relaxation and two computational methods, molecular docking and simulated annealing. The dissociation constant of the CPO−indole complex and the distances between the protons of indole and the heme iron of CPO were obtained. The effect of pH and halide ion on the binding of indole with CPO is presented. Simulated annealing and molecular docking of indole in the active center of CPO are provided. Our results showed that a complex with a K_D of approximately 21 mM is formed between CPO and indole with indole's 2-H pointing toward the heme iron. This structural feature satisfactorily explains the unusual product observed from CPO-catalyzed oxidation of indole. We conclude that formation of the CPO−indole complex is responsible for the escorted delivery of oxygen from CPO compound I directly to position 2 of indole.

MATERIALS AND METHODS

Materials. *C. fumago* (ATCC 16373) was purchased from ATCC (Manassas, VA). Unless otherwise specified, all chemicals were of analytical grade and were purchased from Sigma-Aldrich (St. Louis, MO).

Chloroperoxidase Expression and Purification. CPO was isolated and purified according to published protocols,[38,39] with slight modifications. CPO preparations with Reinheitszahl values (Rz, A_{398}/A_{278} ratios) of ≥1.4 were used. The stock solution of CPO was prepared by repetitive (more than six times) isotope exchange of the aqueous protein solution with D_2O in a Centriprep-30 centrifugal filter device. The concentration of CPO was determined by measuring the absorption at 398 nm using a molar extinction coefficient of 9.12×10^4 M^{-1} cm^{-1}.[1]

Preparation of Stock Solutions and NMR Samples. A stock solution of indole (14.0 mM) was prepared by dissolving 32.8 mg of indole in 20.0 mL of warm D_2O in a vortex mixer. Stock solutions of 1.0 M chloride and iodide ion were prepared from their potassium salts in D_2O. Solutions of 1.0 and 0.1 M DCl were prepared by dissolving DCl [35% (w/w)] in D_2O to adjust the pH of all test solutions. The samples used for NMR experiments contained 2−12 mM indole and 0.1 (or 0.01) mM CPO in 100 mM phosphate buffer with 99.9% D_2O. The final volume of all NMR samples was 500 μL.

Structural Characterization of Indole by NMR. Proton NMR measurements were taken on a Bruker Avance 600 MHz NMR spectrometer at 298.0 K. Proton chemical shifts were referenced to the internal reference 4,4-dimethyl-4-silapentane-1-sulfonic acid (DSS). The NMR data were processed using Topspin, version 2.1. The line width was obtained from proton spectra by fitting the proton peak to a Lorentzian line shape.

T_1 Relaxation Experiments. The longitudinal relaxation time (T_1) was determined using the standard inversion−recovery method with a 180°−τ−90° pulse sequence.[40] Eleven spectra were recorded for each sample, with the interpulse

dx.doi.org/10.1021/bi4002437 | *Biochemistry* 2013, 52, 3688−3701

delay τ ranging from 0.5 to 25.0 s. For each spectrum, 32 scans were acquired. The T_1 values were calculated by fitting eq 1

$$M_Z = M_0(1 - \rho e^{-\tau/T_1}) \quad (1)$$

where τ is the interval between 180° and 90° pulses, M_Z is the Z component of nuclear magnetization (represented by the intensity of the peak) when the interval is τ, M_0 is the Z component of the nuclear magnetization when the interval is infinite, and ρ is a parameter that equals 2.0 at an exactly 180° pulse.

Dissociation Constants of the CPO−Indole Complex. The longitudinal relaxation rate (T_{1obs}^{-1}) is the weighted average of the relaxation rates of the free substrate (T_{1f}^{-1}) and the bound substrate (T_{1b}^{-1}).[41] Thus, the relaxation time values (T_{1obs}^{-1}, T_{1f}^{-1}, and T_{1b}^{-1}) are related as shown in eq 2 when only one molecule of substrate binds to a molecule of enzyme

$$E_0\left(\frac{1}{T_{1obs}} - \frac{1}{T_{1f}}\right)^{-1} = S_0\left(\frac{1}{T_{1b}} - \frac{1}{T_{1f}}\right)^{-1} + K_D\left(\frac{1}{T_{1b}} - \frac{1}{T_{1f}}\right)^{-1} \quad (2)$$

where T_{1obs} is the relaxation time of the indole obtained from the relaxation experiment, T_{1f} is the relaxation time of indole obtained from the relaxation experiment in the absence of CPO, T_{1b} is the relaxation time of the CPO-bound indole, K_D is the dissociation constant of the CPO−indole complex, E_0 is the initial CPO concentration, and S_0 is the initial indole concentration.

Location of the Indole Binding Site. The location of indole in the active site of CPO can be determined from the distances (r) between indole protons and the heme iron of CPO calculated according to the Solomon−Bloembergen equation (eq 3)[24,27,42]

$$\frac{1}{T_{1m}} = \frac{2}{15}\left(\frac{\mu_0}{4\pi}\right)^2 \frac{\gamma^2 g^2 \mu_B{}^2 S(S+1)}{r^6}\left[\frac{\tau_c}{1 + (\omega_I - \omega_S)^2\tau_c{}^2} + \frac{3\tau_c}{1 + \omega_I{}^2\tau_c{}^2} + \frac{6\tau_c}{1 + (\omega_I + \omega_S)^2\tau_c{}^2}\right] \quad (3)$$

where μ_0 is the permeability of free space, γ is the gyromagnetic ratio of the proton, g is the electronic g factor, μ_B is Bohr magneton, S is the spin state of the heme iron of CPO, ω_I and ω_S are the nuclear and electronic Larmor frequencies, respectively, r is the distance from proton nuclei to the heme iron, and τ_c is the correlation time that describes the dipolar interaction between the ligand and the paramagnetic iron in solution. A τ_c value of 8.8×10^{-11} s was used for CPO.[29] When the observed proton is under the extreme narrowing conditions ($\omega_I{}^2\tau_c{}^2 \ll 1$, or $\omega_S{}^2\tau_c{}^2 \gg 1$), as is usually the case for high-spin hemoproteins,[29,43] eq 3 is simplified to eq 4, which was used in calculating the distances in this work.

$$r\ (\text{cm}) = [(8.66 \times 10^{-31})T_{1m}\tau_c]^{1/6} \quad (4)$$

Additionally, T_{1m} is related to T_{1b} through eq 5

$$\frac{1}{T_{1b}} - \frac{1}{T_{1d}} = \frac{1}{T_{1m} + \tau_M} \quad (5)$$

where T_{1d} is the relaxation time in diamagnetic states, T_{1m} is the relaxation time in paramagnetic states, and τ_M is the lifetime of the enzyme−substrate complex. Because both T_{1d} and τ_M are negligible compared to T_{1b} in our case,[23,28,29] T_{1b} is approximately the same as T_{1m}.

Molecular Docking. Molecular docking for the preferred orientation of indole and 1-methylindole within the active site of CPO was performed with AutoDock,[44] version 4.2.3. The results from molecular docking studies provided the starting position of indole for distance-restrained simulated annealing. The structure of CPO for docking indole and 1-methylindole was taken from the X-ray structure (PDB entry 2CPO). Additionally, 14 of the glycosylation sites were removed from the CPO structure, and the pyroglutamic acid (Pca) residue was replaced with a proline residue, because parameters for sugars and the Pca residue are unavailable in the GROningen MOlecular Simulation (GROMOS) force field[45] that was used in our simulated annealing. The removal of sugars from CPO should have a negligible effect on substrate binding, because CPO without glycosylation is still highly active.[46] Furthermore, the manganese ion was removed from the CPO structure, as manganese-free CPO[47] was used in our NMR experiment. The crystallographic water in the PDB file was removed to reduce any interference from that water during docking.

Both the indole and 1-methylindole structures were built by MarvinSketch, version 5.9, in the JChem software package (ChemAxon, Ltd.) and further optimized with ORCA,[48] version 2.9, using second-order Møller−Plesset perturbation theory (MP2)[49] and the def2-SVP basis set.[50] AutoDockTools,[51] version 1.5.4, was used to add Gasteiger charges to CPO (+1.00 was added manually on Fe), indole, and 1-methylindole. During simulation, the CPO structure was kept rigid. Indole or 1-methylindole was simulated in a box centered at the heme iron, which was confined using a grid size of 30 Å × 30 Å × 30 Å with 0.375 Å spacing. Docking consisting of 60 separate simulation runs was performed with 25 million energy evaluations per run.

Distance-Restrained Simulated Annealing. Distance-restrained simulated annealing and energy minimization for the CPO−indole complex were performed with Groningen MAchine for Chemical Simulation (GROMACS),[52] version 4.6, using the GROMOS96 53a6 force field.[45] The force field was augmented with the parameters developed in this work (see Table S1 of the Supporting Information). The parameters for indole were built using the PRODRG2 server.[53] The partial atomic charges of indole were assigned by analogy with the equivalent functional group, tryptophan, in the GROMOS96 53a6 force field.[54] The bonded parameters and partial atomic charges for the heme ligated with cysteine were derived using Seminario's method[55] and CHELPG (CHarges from Electrostatic Potentials using a Grid based)[56] method, respectively (see the Supporting Information); the van der Waals parameters were those already in the force field.

The CPO−indole complex was solvated with simple point charge (SPC) waters.[57] The protonation states of the titratable amino acid residues of CPO were assigned as follows: +1 for His and Lys, −1 for Glu and Asp, and neutral for Tyr. The protein has a net charge of −16, so 16 Na^+ ions were added to create a neutral system for simulation. Periodic boundary conditions were imposed using a truncated octahedral box created from an 82 Å × 82 Å × 82 Å cube. After the overlapping waters had been deleted, 12644 waters remained. A shift method with a 14 Å cutoff was used for the calculation of Lennard-Jones interactions. Electrostatic interactions were calculated with the particle mesh Ewald method (PME),[58]

dx.doi.org/10.1021/bi4002437 | Biochemistry 2013, 52, 3688−3701

using a cutoff of 12 Å for real-space interactions, a Gaussian width parameter of 3.84195 Å, an FFT grid determined with the Fourier spacing method using a maximal spacing of 1.2 Å, and fourth-order interpolation for reciprocal-space interactions. A relative dielectric constant (ε_r = 1.0) was used. All bond lengths were constrained using the LINCS algorithm.[59] Positional restraints were placed on the backbone α-carbon during simulated annealing. Indole was restrained with a force constant of 600 kJ mol^{-1} nm^{-2} using the NMR-derived distances between the protons of indole and the heme iron (see Table S2 of the Supporting Information). A time constant of 50 ps was applied to the distance restraint, while the violation of the distance restraint was the square root of the product of the time-averaged violation and the instantaneous violation. Brief energy minimization of CPO–indole complex was performed using the conjugate gradient method to eliminate unrealistic van der Waals contacts. The system was rapidly heated to 800 K, cooled to 300 K over 150 ps, and allowed to equilibrate for 100 ps at 300 K, using a 2 fs time step. The analysis described below is based on Coulomb and Lennard-Jones interaction energies calculated during the last 50 ps, root-mean-square deviations (rmsds) calculated with respect to the starting structure, and snapshots of the indole molecule bound to CPO during the last 50 ps of MD simulation.

RESULTS AND DISCUSSION

Proton NMR Spectrum of Indole in the Presence of CPO. Figure 1 compares the ^{1}H NMR spectra of 5.7 mM indole in the absence (Figure 1A) and presence of varying amounts [0.01, 0.02, 0.05, 0.08, and 0.1 mM (Figure 1B–F)] of CPO at pH 6.0. The six main peaks (Figure 1A) can be easily assigned, based on the splitting pattern and shift positions, to the protons of indole shown in Scheme 1: 7.32 (2-H), 6.51 (3-H), 7.63 (4-H), 7.08 (5-H), 7.17 (6-H), and 7.47 ppm (7-H). 1-H was not observed because of its fast exchange with D_2O. After the addition of CPO, the doublet from 2- and 3-H (Figure 1A) was changed to two broad singlets because of the paramagnetism of the heme in CPO (Figure 1B), suggesting the proximity of these protons to the heme iron. Further increasing the concentration of CPO led to more significant broadening of these peaks (Figure 1B–F). It is also noted that as CPO concentration was increased, all indole resonances became broader, which was coupled with a noticeable shift in their resonance positions (Figure 1B–F). For instance, the chemical shift of 4-H changed from 7.63 to 7.61 ppm. The change in chemical shifts results from the dipole–dipole interaction between indole and the heme iron,[25] while line broadening of the signals is due to paramagnetic enhancements of the transverse nuclear relaxation rates (T_2^{-1}) of indole caused by the heme iron.[25] The results shown in Figure 1 indicate that a reasonably stable CPO–indole complex is formed with indole bound near the heme center of the protein. More importantly, the NMR signal from all indole protons can be clearly observed, making it possible to obtain the orientation of indole in the active center of CPO because multiple distances between substrate protons and the heme iron can be experimentally determined.

As the concentration of CPO increased from 0.01 to 0.05 mM, the line width of the 2-H increased from 2.47 to 54.37 Hz (Figure 1B–D). The peak of 2-H was broadened so severely that it became hardly observable when the concentration of CPO reached ≥0.08 mM (Figure 1E,F). The line width of 3-H also increased dramatically from 4.27 to 59.64 Hz (Figure 1B–F) as the concentration of CPO was increased from 0.01 to 0.1 mM, although the broadening effect was not as profound as that observed for 2-H. In contrast, other peaks were less broadened than those of 2- and 3-H. For instance, the line width of 4-H increased gradually from 4.00 to 15.71 Hz in the CPO concentration range tested (Figure 1B–F). This suggests that protons in the pyrrole ring are closer to the heme iron than protons in the benzene ring of indole, with 2-H being the closest. The systematic broadening of indole proton resonances observed here is consistent with our previous study of the CPO–CPDO complex.[23]

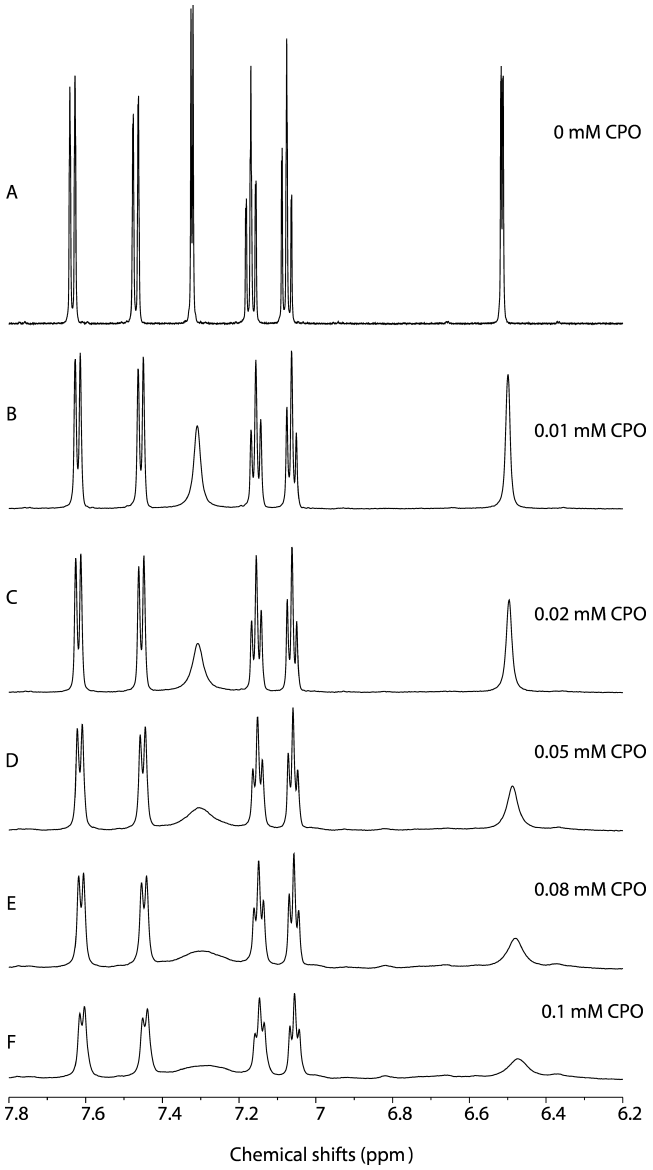

Figure 1. Effect of the concentration of CPO on the proton NMR spectra of indole. The spectra (A–F) were recorded in 10 mM deuterated phosphate buffer (pH 6.0) containing 5.7 mM indole and a fixed concentration of CPO.

Dissociation Constant of the CPO–Indole Complex. To evaluate the binding affinity between CPO and indole, the longitudinal relaxation time (T_1) of indole protons was measured in the presence of 0.1 mM CPO and different concentrations of indole (2.8–11.0 mM) at pH 6.0. Figure 2 shows the nice exponential fit of signal intensities (M_Z) as a function of the delay time (τ) as defined in eq 1, using the

dx.doi.org/10.1021/bi4002437 | Biochemistry 2013, 52, 3688–3701

Scheme 1. CPO-Catalyzed Oxidation of Indole to 2-Oxindole Using H_2O_2[a]

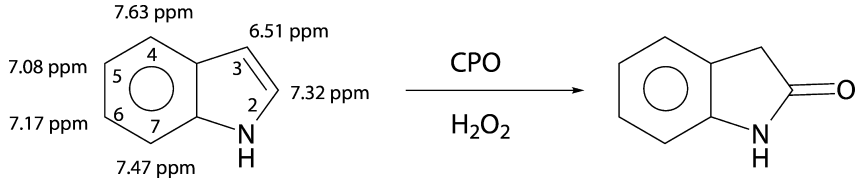

[a]The indole structure is labeled with proton chemical shifts. Proton number assignments are shown.

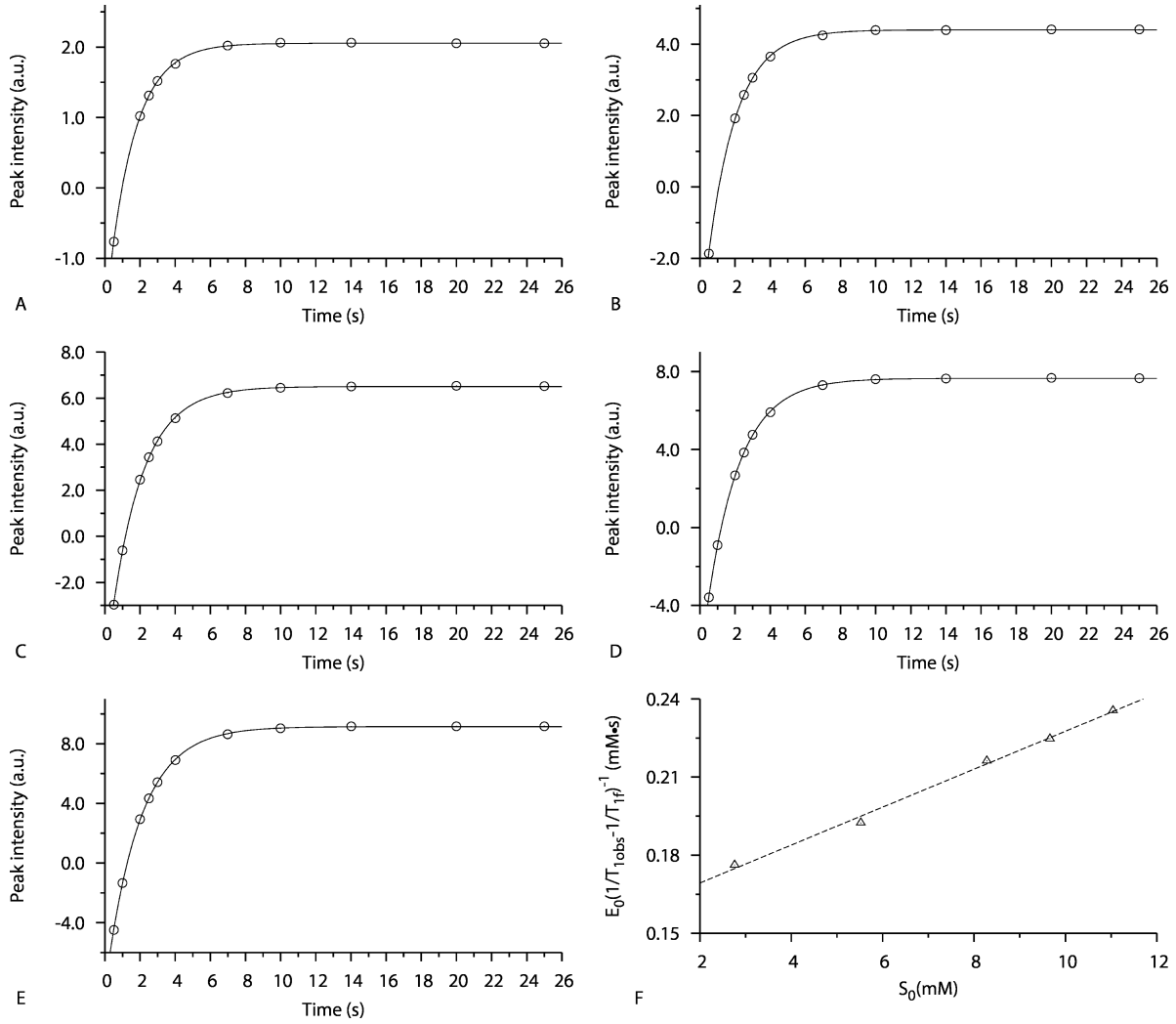

Figure 2. NMR relaxation experiments for 4-H of indole in the presence of CPO. (A–E) Plots of peak intensities at 7.61 ppm as a function of inversion recovery time (τ). The experimental results (dots) were obtained in 100 mM deuterated phosphate buffer (pH 6.0) containing 0.1 mM CPO and (A) 2.8, (B) 5.5, (C) 8.3, (D) 9.7, and (E) 11.0 mM indole. The curves are the exponential fits to eq 1. (F) Plot of $E_0(1/T_{1obs} - 1/T_{1f})^{-1}$ as a function of indole concentration (S_0). The line is the least-squares fit to eq 2 and is used to estimate the K_D.

resonance at 7.61 ppm (4-H) as an example. Similar fits were obtained for other protons of indole (data not shown). Therefore, the T_{1obs} of 4-H (Figure 2A–E) can be obtained from eq 1 (1.51, 1.63, 1.79, 1.85, and 1.92 s, respectively). The increase in T_{1obs} is attributed to the increase in the fraction of free indole as its concentration is increased.

Figure 2F shows a plot of $E_0(1/T_{1obs} - 1/T_{1f})^{-1}$ versus S_0 for 4-H. The fitted straight line demonstrates the reliability of the data (R^2 = 0.9957). The K_D value can be calculated as the intercept of the fitted line divided by its slope using eq 2. The K_D calculated from Figure 2F was approximately 21 mM as listed in Table 1. This value is dramatically different from the K_M (3.3 mM) for CPO-catalyzed oxidation of indole.[60] The inconsistency between K_D and K_M is most probably due to the fact that K_M is affected by many species involved in the entire catalytic process, while K_D is soly determined by the stability of the enzyme–substrate complex. A K_D higher than K_M has been observed for complexes between CPO and other substrates.[23] To verify the results from our NMR studies, we also studied the K_D value for the CPO–indole complex using difference optical absorption techniques. Results of our UV–vis studies are in good agreement with those derived from our NMR studies (data not shown).

dx.doi.org/10.1021/bi4002437 | *Biochemistry* 2013, 52, 3688–3701

Table 1. Dissociation Constants (K_D) of the CPO−Indole Complex and Distances (r) between the Protons of Indole and CPO Heme Iron[a]

position	δ (ppm)	T_{1b} (s)[b]	r (Å)	K_D (mM)
2-H	7.31	6.8×10^{-5}	4.2	21
3-H	6.50	3.7×10^{-4}	5.5	26
4-H	7.61	7.2×10^{-3}	9.1	21
5-H	7.06	1.6×10^{-2}	10.4	22
6-H	7.15	1.8×10^{-2}	10.5	20
7-H	7.44	9.9×10^{-3}	9.5	19

[a]The relaxation experiments were performed in 10 mM deuterated phosphate buffer (pH 6.0) containing 0.01 mM CPO to measure the δ and T_1 of 2- and 3-H or 0.1 mM CPO for the other protons by changing the indole concentration from 2.8 to 11.0 mM. [b]The average was from two independent experiments.

Figure 3 shows plots of $E_0(1/T_{1obs} - 1/T_{1f})^{-1}$ versus S_0 for other protons. All correlation values of the fits (R^2) were higher than 0.98. It should be noted that linear fits could only be obtained for 2- and 3-H in the presence of 0.01 mM CPO. Protons in the benzene ring of indole did not give reliable results in a 0.01 mM CPO solution and thus do not fit into eq 2 possibly because of the weak paramagnetic effect at low enzyme concentrations and long distances from these protons to the heme iron. Therefore, a higher concentration of CPO (0.1 mM) was used to measure the relaxation rates of protons on the benzene ring of indole. Table 1 lists the dissociation constants (K_D) of the CPO−indole complex at pH 6.0. The K_D values obtained from the relaxation property of different protons in indole are quite consistent, further proving the validity of the relaxation method in probing the structural properties of heme protein−substrate complexes. The average of K_D values calculated from all protons of indole is ~21 mM, indicating a weak binding of indole to CPO. This value is comparable to the reported K_D of 33 mM for the binding of CPDO to CPO.[23] The stability of the CPO−indole complex also compares nicely with that of the indole−P450 BM3 complex.[61]

Distances between the Heme Iron and the Protons of Indole. To reveal the orientation of indole in the active site of CPO, we used paramagnetically induced NMR relaxation of indole in the presence of CPO to calculate the distance between the heme iron and the protons of indole. Table 1 lists the NMR relaxation times, $T_{1b,}$ and the calculated distances between the protons of indole and the heme iron of CPO. These distances are consistent with those obtained for alky phenyl sulfides (8.0−10.9 Å),[29] phenols (5.6−9.3 Å),[28] and

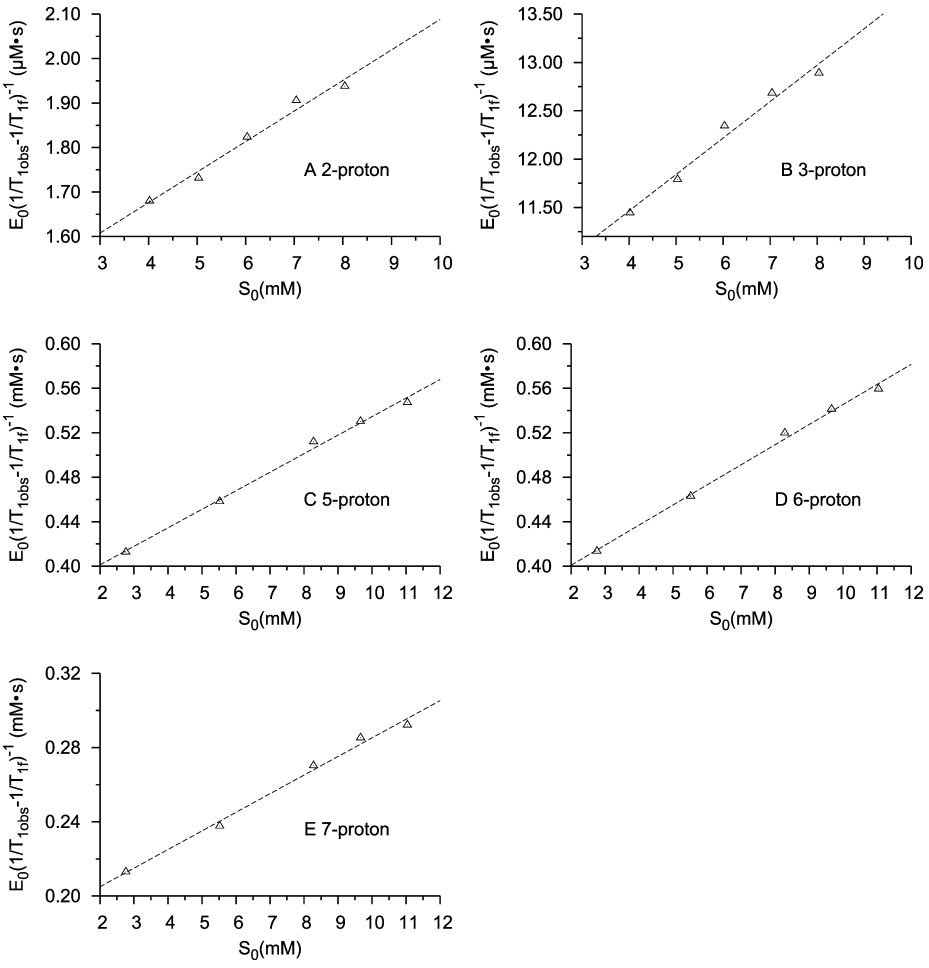

Figure 3. Plots of $E_0(1/T_{1obs} - 1/T_{1f})^{-1}$ as a function of indole concentration (S_0) for (A) 2-H, (B) 3-H, (C) 5-H, (D) 6-H, and (E) 7-H of indole. The relaxation experiments were conducted in (A and B) 10 mM deuterated phosphate buffer containing 0.01 mM CPO and various indole concentrations or (C−E) 100 mM deuterated phosphate buffer containing 0.1 mM CPO and various indole concentrations. To plot the label on the y-axis clearly, $E_0(1/T_{1obs} - 1/T_{1f})^{-1}$ values of panels A and B were plotted in units of micromolar per second.

dx.doi.org/10.1021/bi4002437 | *Biochemistry* 2013, 52, 3688−3701

CPDO (7.1 Å)[23] binding to CPO. Examination of Table 1 reveals that the pyrrole ring of indole is closer than the benzene ring to the heme iron. The distance between the heme iron of CPO and the 2-H of indole is the shortest. This position happens to be the location at which C−H oxidation takes place, indicating that the oxidation of indole proceeds by a direct insertion of oxygen from the oxyferryl intermediates of CPO. Furthermore, the use of these distance constraints (Table S2 of the Supporting Information) in advanced computational methods such as simulated annealing[62,63] can provide the precise orientation and position of indole in the active site of CPO, which will be presented in Distance-Restrained Model of CPO Complexed with Indole.

Effect of pH on the Binding of Indole to CPO. To check the effect of pH on the binding of indole to CPO, the K_D and the distances from 2- and 3-H to the heme iron were determined in the pH range of 3.0−6.5 because of the stability restriction of CPO (Table 2). It has been reported that in the absence of hydrogen peroxide, CPO is stable up to pH 6.5.[64,65] The relaxation time of 3-H of indole cannot be determined at pH ≤4.0 because of acid-catalyzed tautomerization of the N-protonated species[66] that leads to the exchange of 3-H with deuterated solvent. Therefore, the K_D values listed in Table 2 were derived from T_1 of 2-H only. Surprisingly, both the dissociation constant, K_D, and the distance, r, between 2-H of indole and CPO heme iron were independent of pH in the pH range tested (Table 2), indicating that no ionizable group is involved in the binding of indole to CPO. This is in conflict with the fact that the activity of CPO-catalyzed oxidation of indole is strongly pH dependent. Like most heme peroxidases, CPO uses compound I rather than the resting state enzyme itself to oxidize substrates. Therefore, our results imply that the effect of pH on CPO's catalytic activity is primarily due to changes in the rate of formation of CPO compound I rather than the formation of CPO−substrate complexes, especially for hydrophobic organic substrates. It should be noted that the observed pH inertness of binding of indole to CPO is also at odds with the case of CPDO in which an ionizable group with a pK_a between 4.5 and 6.5 is involved in the formation of the CPO−CPDO complex.[23] The ionizable group has been suggested to be either a carboxylate residue (Glu183) or a histidine imidazole group (His105).[23] Because CPDO is polar, it may require hydrogen bonding with Glu183 or His105 to stabilize its binding with CPO. In contrast to CPDO, indole is neutral and hydrophobic; therefore, its binding with CPO would naturally be dominated by hydrophobic interactions with the enzyme. The X-ray structure of CPO has revealed the presence of a putative hydrophobic channel for the approach of organic substrates to the heme active site.[22] At the bottom of this hydrophobic channel, two phenylalanines, Phe103 and Phe186, serve as the gatekeeper in controlling the substrate selectivity of CPO. Therefore, these two residues are likely to be the principal contact sites for the hydrophobic interactions between CPO and indole.

Table 2. Dissociation Constants (K_D) of the CPO−Indole Complex and Distances (r) between the Protons of Indole and the CPO Heme Iron[a] at Different pH Values

	T_{1bs} (s)		r (Å)		
pH	2-H	3-H	2-H	3-H	K_D (mM)[c]
3.0	7.0×10^{-5}	nd[b]	4.2	nd[b]	25
3.5	5.6×10^{-5}	nd[b]	4.0	nd[b]	25
4.0	6.2×10^{-5}	nd[b]	4.1	nd[b]	23
4.5	5.6×10^{-5}	3.2×10^{-4}	4.0	5.4	25
5.0	6.0×10^{-5}	4.1×10^{-4}	4.1	5.6	23
5.5	6.1×10^{-5}	3.8×10^{-4}	4.1	5.5	23
6.0	6.8×10^{-5}	3.7×10^{-4}	4.2	5.5	21
6.5	6.0×10^{-5}	4.1×10^{-4}	4.1	5.6	23

[a]The relaxation experiments were performed in 10 mM deuterated phosphate buffer (pH 3.0−6.5) containing 0.01 mM CPO to measure the T_1 values of 2- and 3-H by changing the indole concentration from 2.0 to 12.0 mM. [b]Not determined because of deuterated exchanged of 3-H. [c]The dissociation constants were derived from relaxation experiments with 2-H.

Association of Indole with CPO in the Presence of Halide Ion. It is well-known that halides (including chloride, bromide, and iodide) are cosubstrates of CPO-catalyzed halogenations.[3] Although CPO from *C. fumago* is incapable of catalyzing the halogenation of indole, halide binding sites have indeed been identified in a recent X-ray diffraction study of CPO.[62] To probe the effect of chloride and iodide on the binding of indole to CPO, the K_D and the distances from 2- and 3-H to the heme iron in the presence of chloride and iodide were measured. Both K_D and the distances displayed a negligible dependence on the presence of chloride and iodide (Tables 2 and 3), indicating that chloride and iodide do not affect the binding affinity of indole for or the orientation of indole with respect to CPO. This is consistent with the previous report of the CPO−CPDO complex in the presence of chloride ion[23] and is supported by the absence of chloride binding sites in chloride-soaked crystals of CPO.[2,22] However, the essentially identical K_D of the CPO−indole complex in the presence of varying concentrations of iodide is somewhat surprising as CPO does have three iodide binding sites at the distal heme pocket.[22] The effect of iodide on substrate binding

Table 3. Dissociation Constants (K_D) of the CPO−Indole Complex and Distances (r) between the Protons of Indole and CPO Heme Iron[a] in the Presence of Chloride or Iodide Ion

	T_{1bs} (s)		r (Å)		
	2-H	3-H	2-H	3-H	K_D (mM)[b]
		pH 6.0			
10 mM Cl^-	6.5×10^{-5}	4.2×10^{-4}	4.1	5.6	24
20 mM Cl^-	5.5×10^{-5}	3.4×10^{-4}	4.0	5.4	25
30 mM Cl^-	5.6×10^{-5}	3.4×10^{-4}	4.0	5.4	24
40 mM Cl^-	6.2×10^{-5}	3.4×10^{-4}	4.1	5.4	22
		pH 4.0			
20 mM Cl^-	7.1×10^{-5}		4.2		20
		pH 6.0			
10 mM I^-	6.6×10^{-5}	3.8×10^{-4}	4.1	5.5	25
20 mM I^-	6.4×10^{-5}	3.4×10^{-4}	4.1	5.4	20
30 mM I^-	5.4×10^{-5}	4.0×10^{-4}	4.0	5.6	26
40 mM I^-	6.8×10^{-5}	3.7×10^{-4}	4.1	5.5	21
		pH 4.0			
20 mM I^-	8.6×10^{-5}		4.3		20

[a]The relaxation experiments were performed in 10 mM deuterated phosphate buffer (pH 4.0 and 6.0) containing 0.01 mM CPO and a certain concentration of chloride or iodide ion to measure the T_1 of 2- and 3-H by changing the indole concentration from 2.0 to 12.0 mM. [b]The dissociation constants were evaluated from relaxation experiments with 2-H.

dx.doi.org/10.1021/bi4002437 | *Biochemistry* 2013, 52, 3688−3701

was confirmed by our previous study of the CPO−CPDO complex, which displayed a dramatic increase in K_D (from 33 to 123 mM) as the concentration of iodide was increased.[23] This was later rationalized by possible steric clashes between CPDO and CPO-bound iodide, because the distance between the carbonyl oxygen of CPDO and CPO-bound iodide is only 1.9 Å.[22] It is thus proposed that the effect of iodide ion on the binding of substrates to CPO depends on the specific structure and nature of the substrates. Substrates such as CPDO that undergo halogenation reactions are affected by the presence of iodide, while substrates undergoing other transformations are not, implying that iodide binding results in little or no structural rearrangement for the substrate binding site of CPO. For CPO-catalyzed chlorination reactions, chloride ion is captured by compound I[67,68] without the need for a bound chloride ion at the active site of CPO. This is plausible because the physiological environment in which CPO functions has sufficient chloride ion to satisfy its need for chlorination reactions.

Molecular Docking Models of Indole Bound to CPO. As a first step in determing the preferred orientations of indole within the active site of CPO, computer-aided docking of the molecules including indole and its *N*-methyl derivative into the active site of CPO was performed. During 60 Autodock runs, only one cluster of poses for indole (or its derivative) was observed. The key issue described here is the position and orientation of the substrate with respect to the heme and Glu183 in the active site of CPO, because Glu183 is postulated to be the acid−base catalyst in compound I formation[69,70] and thus to tune the catalytic activity of CPO.[71] Figure 4A shows the CPO−indole complex deduced from molecular docking. The pyrrole ring of indole faces the heme, with 2-H being the closest to the heme iron. The orientation of indole observed here is consistent with that derived from the distances between the protons of indole and the heme iron in our relaxation experiments (Table 1). Additionally, the NH group of indole is 1.7 Å from the γ-carboxyl group of Glu183, indicating that, potentially, a hydrogen bond can be formed between the NH group of indole and Glu183. This hydrogen bond, even if it does form, is not sufficient to be the major factor in keeping indole in its binding site in CPO.[36] However, it is reported that the hydrogen bond between Glu183 and the alcoholic OH group directs benzyl alcohol or 2-phenylethanol to a specific orientation.[72] To further elucidate the function of a hydrogen bond formed between the NH group of indole and Glu183, 1-methylindole was also docked into the active site (Figure 4B). It is observed that the methyl group of 1-methylindole points toward the heme, not Glu183. Thus, the orientation of 1-methylindole is different from that of indole within the active site of CPO (Figure 4A). This is attributed to both the hindrance caused by a bulkier methyl group and the disruption of the putative hydrogen bond between indole and Glu183. This also confirms that the NH group of indole does play a role in the binding of indole to CPO, because 1-methylindole is indeed hardly oxidized by CPO.[36] Therefore, the observed negligible effect of pH on the K_D of the CPO−indole complex from our NMR relaxation studies can be attributed to the extremely low pK_a of Glu183 within the active site of CPO.

The binding energy, which is the free energy released by the formation of the complex between the substrate and the enzyme, is an important parameter for evaluating the bioaffinity of the substrate for the enzyme.[73] The docking study resulted in binding energies of −23.2 kJ/mol for the CPO−indole complex and −21.9 kJ/mol for the CPO−1-methylindole complex. Compared to the binding of substrates to P450, such as indole (−53.5 kJ/mol)[74] and ticlopidine (−32.6 kJ/mol),[75] the binding of indole to CPO is apparently weaker. This agrees with the conclusion from our NMR relaxation experiments (Table 1). The slightly smaller (in magnitude) binding energy for binding of 1-methylindole to CPO relative to that of indole can be partly attributed to the loss of a hydrogen bond with Glu183.

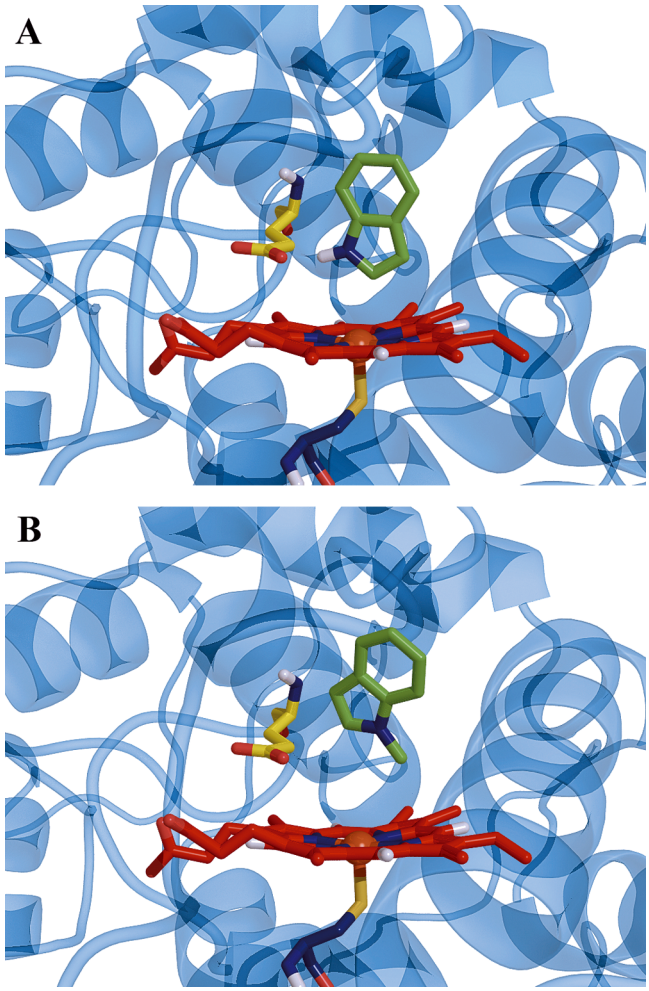

Figure 4. Ribbon and stick representations of (A) indole and (B) 1-methylindole docking in the active site of CPO. There was only one orientation of indole and 1-methylindole found in docking. Indole and 1-methylindole are colored green. Heme is shown as red sticks, and Glu183 is shown as yellow sticks.

Distance-Restrained Model of CPO Complexed with Indole. To further investigate the interaction between indole and CPO, simulated annealing of the CPO−indole complex was performed using the distances calculated from our NMR relaxation studies at pH 5.0 (Table S2 of the Supporting Information). Mean interaction energies of CPO with indole were calculated for the last 50 ps of the simulated annealing. The root-mean-square deviation (rmsd) of the coordinates of CPO in the CPO−indole complex relative to the crystal structure reaches a constant value (~1.4 Å) in the last 50 ps, indicating stability of the CPO−indole complex. Figure 5 depicts the structural model of indole in the active site of CPO deduced from simulated annealing. Ten equally spaced snapshots from the last 50 ps of simulation are overlaid. The

dx.doi.org/10.1021/bi4002437 | *Biochemistry* 2013, 52, 3688−3701

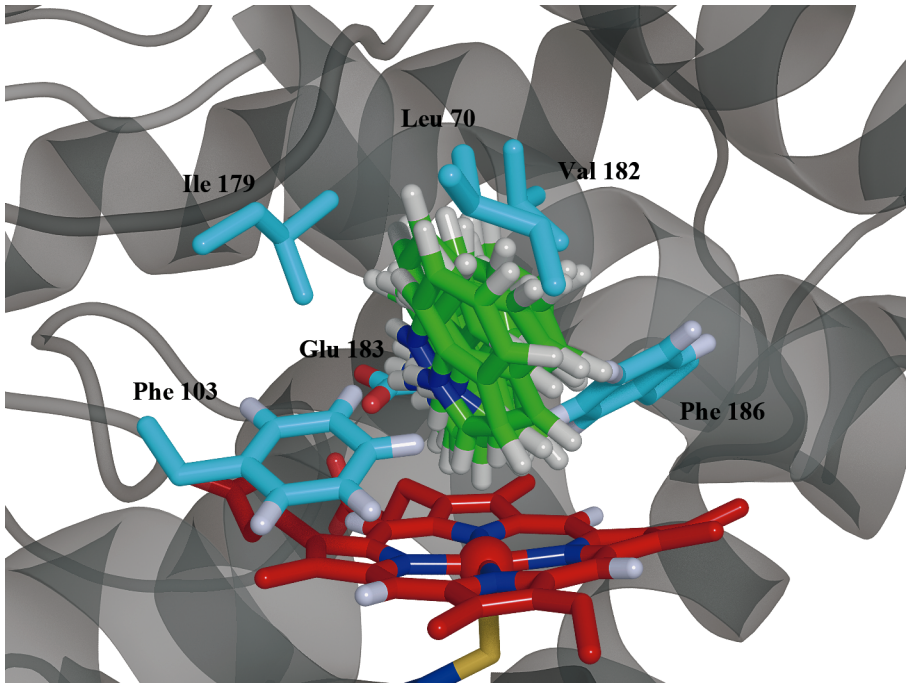

Figure 5. Distance-restrained model of indole in the active site of CPO. The residues within 5 Å of indole are Val67, Ile68, Leu70, Ala71, Asn74, Phe103, Ile179, Val182, Glu183, Phe186, and Ala267. The side chains of Leu70, Phe103, Ile179, Val182, Glu183, and Phe186 are shown for the sake of clarity. To differentiate the protein residues from the substrate, the indole molecules are colored green, the heme is colored red, and the carbons of the residues are colored blue.

orientation of the indole is seen to be quite stable. The distances between the protons of indole and the heme iron observed in Figure 5 are ~2 Å shorter than those of the NMR results (Table S2 of the Supporting Information). This is consistent with previous results in which the distances between the protons of CPDO and the heme iron of the crystal structure of a CPO−CPDO complex[22] (4.9 Å) are much shorter than those of a relaxation measurement[23] (7.1 Å). Furthermore, differences between distances obtained with the distance-restrained model and the NMR results are also observed in a study of the CYP1A1−phenacetin complex.[76] Such differences may be attributed to the fact that NMR results reflect an ensemble of multiple orientations of the substrate in the active site.[75] In spite of such an ensemble, there should be only one major indole orientation as indicated by the significant broadness of NMR peaks of 2- and 3-H of indole compared to other protons (Figure 1). Therefore, the distance-restrained model investigated here should be sufficient for studying the mechanism of regioselective oxidation catalyzed by CPO. It is observed that the residues within 5 Å of indole are Val67, Ile68, Leu70, Ala71, Asn74, Phe103, Ile179, Val182, Glu183, Phe186, and Ala267. The side chain rmsds of these residues, except for Glu183, averaged over the last 50 ps are comparable to the corresponding root-mean-square fluctuations (rmsfs) (see Table S3 of the Supporting Information). The rmsd of Glu183 turned out to be much larger than the corresponding rmsf, suggesting that the substantial adjustment of the orientation of the charged Glu183 side chain is a prerequisite for binding of indole at the active site. This is consistent with a previous study[71] that showed that Glu183 mobility is critical for the catalytic reactivity of CPO. Furthermore, the residues in the active site strongly interacting with indole are critically important; identification of these residues can serve as a lighthouse for designing better CPO mutants for the oxidation of not only indole but also similar types of organic substrates. Therefore, the interaction energies between the active site residues and the indole molecule were examined (Table S4 of the Supporting Information).

The calculated Coulomb and Lennard-Jones potential energies of indole bound to CPO (Table S3 of the Supporting Information) can be interpreted as representing electrostatic and hydrophobic interactions, respectively. A strong Coulomb interaction (−25.7 kJ/mol) was found between indole and Glu183, indicating the presence of a hydrogen bond between the bound substrate and Glu183. This agrees with our molecular docking studies of this system. His105 in CPO has been postulated to form a hydrogen bond with and modulate the acidity of Glu183.[77,78] The interaction between His105 and Glu183 helps hold Glu183 in its place to interact with iron-bound hydrogen peroxide that facilitates the formation of compound I. It has been demonstrated that chemical modification of His105 is detrimental to CPO-catalyzed oxidations.[79] To learn whether His105 can affect the binding of indole to CPO, we evaluated the interaction between His105 and indole. It was found that only a weak repulsive Coulomb interaction (4.3 kJ/mol) exists between His105 and indole, indicating that His105 has little direct effect on the binding of indole to CPO, although His105 can indirectly influence indole binding via its effect on the orientation and pK_a of Glu183. Additionally, a weak Coulomb interaction (−2.1 kJ/mol) was found between indole and Va 67. Surprisingly, the Coulomb interaction between indole and Asn74 was also weak (−1.2 kJ/mol), indicating that the interaction between Asn74 and indole is not essential for substrate binding. This is quite different from the case of polar substrates such as ethylene glycol and dimethyl sulfoxide, which interact with Asn74 extensively.[22]

The van der Waals interaction (−103 kJ/mol) was much stronger than the Coulomb interaction between CPO and

dx.doi.org/10.1021/bi4002437 | *Biochemistry* 2013, 52, 3688−3701

Scheme 2. Proposed Mechanism of CPO-Catalzyed Oxidation of Indole

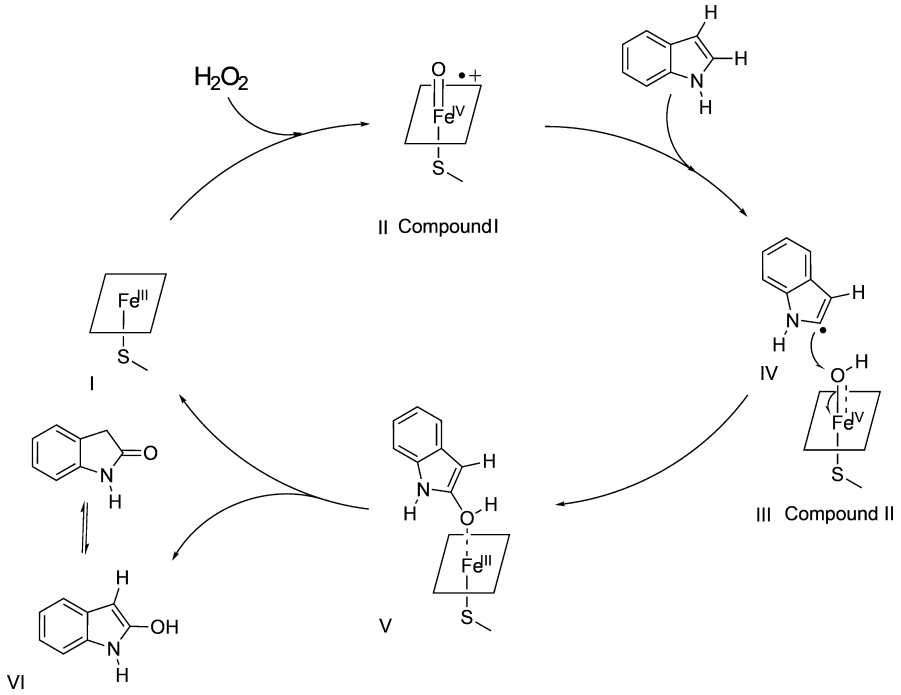

indole (−30 kJ/mol) from our simulated annealing studies. This indicates that the formation of the CPO−indole complex is mainly governed by hydrophobic interaction, rather than hydrogen bond or electrostatic interactions. Specifically, indole interacts strongly with several key hydrophobic residues, including Leu70, Phe103, Ile179, Val182, and Phe186 at the active center of CPO. These residues contribute −6.6 to −10.4 kJ/mol per residue to the formation of the CPO−indole complex (see Table S4 of the Supporting Information). This agrees with reports that these hydrophobic residues interact significantly with hydrophobic substrates such as *cis*-*β*-methylstyrene[71,80] and anthracene.[81]

This structural model (Figure 5) is in good agreement with the fact that the catalytically active form of CPO is a compound I intermediate with O as the axial ligand. Assuming an Fe−O bond length of 1.65 Å in CPO compound I[82] and the structure of the CPO−indole complex derived from the distance-restrained model remain essentially unchanged after formation of compound I, the distance between oxoferryl oxygen and 2-C of indole would be ∼2.6 Å. This short distance agrees with the direct transfer of oxygen to the oxidation site (2-C) of indole. Although the flexibility of CPO's distal pocket is important for tuning the catalytic reactivity of CPO,[71] the assumption of the same structure may hold as the crystal structures of the CPO−ligand adduct[21] and the hydroperoxo-ferric intermediate, compound 0,[83] are indistinguishable from that of CPO. Furthermore, the binding of substrates should weaken the Fe−O bond in the transition state, ensuring the efficient transfer of O from compound I to the substrate, as demonstrated by the elongation of the Fe−O bond in the oxidation of dimethyl sulfide by compound I of cytochrome P450.[84]

Mechanism of CPO-Catalyzed Oxidation of Indole. On the basis of our NMR relaxation measurements and the distance-restrained models presented in Figure 5, a mechanism for CPO-catalyzed regioselective oxidation of indole is proposed (Scheme 2). As for all CPO-catalyzed reactions, the oxidation of indole is initiated by the binding of a neutral hydrogen peroxide molecule to the heme iron of CPO [Fe^{III} (Scheme 2, I)]. Binding of H_2O_2 to the heme iron is facilitated by the transfer of one of the peroxide hydrogens to the carboxyl oxygen of Glu183.[2] The hydrogen ion is then delivered to the distal oxygen of the peroxide as the peroxide bond is heterolytically cleaved to produce an oxoferryl *π*-cation radical intermediate [Fe^{IV}═$O^{•+}$ (Scheme 2, II)] known as compound I. Formation of compound I has been observed and characterized through many different techniques, including electron paramagnetic resonance (EPR),[85] Mössbauer,[85] X-ray absorption,[82] and electron nuclear double-resonance spectroscopy.[86] Single-electron reduction of compound I by indole converts compound I to compound II (Scheme 2, III)[87] and generates an indole radical intermediate (Scheme 2, IV). The presence of substrate intermediates as carbon-centered radicals has been established in P450-catalyzed reactions.[88] Additional evidence in favor of such a radical intermediate is provided by EPR studies of lactoperoxidase in the sulfoxidation[89] and by ^{1}H NMR and EPR studies of a synthetic heme system in the epoxidation of styrene.[90] In addition, the hydrogen atom abstraction of the substrate is also presumed to be the mechanism in CPO-catalyzed demethylation of *N*,*N*-dimethylanilines.[91] Bukowski et al.[92] and Green[93] suggested that the abstraction of a hydrogen atom from reducing substrates is facilitated by the axial thiolate ligand. Reduction of compound II results in the transfer of the ferryl oxygen to the substrate and the regeneration of the initial ferric resting state of CPO. Consequently, 2-hydroxyindole is formed (Scheme 2, V), which spontaneously tautomerizes to the stable oxindole (Scheme 2, VI). Similar mechanisms have been reported in CPO-catalyzed oxidative dehalogenation.[94] Furthermore, our results clearly indicate that the consecutive electron transfers occur between position 2 of indole and CPO intermediates, because 2-H of indole is pointing directly to the heme iron. Therefore, CPO-catalyzed oxidation of indole has a regioselectivity at position 2.

dx.doi.org/10.1021/bi4002437 | *Biochemistry* 2013, 52, 3688−3701

CONCLUSION

This work provides insights into the mechanism of CPO-catalzyed regioselective oxidation of indole. Association of indole with CPO was confirmed from both line width and longitudinal relaxation time measurements of the proton NMR signals of indole. Significantly, the precise orientation of indole in the CPO heme cavity was deduced from our results. The dissociation constant of the CPO−indole complex was calculated to be ∼21 mM, and the distances between protons of indole (2-, 3-, 4-, 5-, 6-, and 7-H) and the heme iron of CPO were 4.3, 5.6, 9.2, 10.5, 10.7, and 9.7 Å, respectively. In the pH range of 3.0−6.5, the dissociation constant of the CPO−indole complex and the position of indole in the active site are independent of solution pH. It was also found that the presence of halide (chloride and iodide) ion negligibly affects the stability of the CPO−indole complex and the binding geometry of indole in the active site of CPO at pH 6. Molecular docking of indole into the active site of CPO revealed that the pyrrole ring of indole points to the heme and 2-H of indole is the closest to the heme iron, confirming the results from NMR studies of the CPO−indole complex. This indicates a direct insertion mechanism for insertion of oxygen into the C−H bond at position 2 of indole and provides the first experimental explanation for the "unusual" regioselectivity of CPO-catalyzed oxidation of indole. On the other hand, molecular docking of 1-methylindole reveals that the methyl group points toward the heme iron, not Glu183 as in the case of indole. These docking studies suggest that the NH group of indole plays an important role in the binding of indole to CPO. The observed pH independence of binding of indole to CPO in our pH effect experiments may be attributed to the low pK_a of Glu183, which remains fully deprotonated within the pH range tested in our experiments. Furthermore, simulated annealing of the CPO−indole complex indicates that the Coulombic interaction between indole and Glu183 is much stronger than that among Val67, Asn74, and His105. Finally, our study demonstrated that the association of CPO with indole is mainly governed by hydrophobic interactions rather than electrostatic interactions. This work provides the first experimental and theoretical explanation for the observed "unexpected" regioselectivity of CPO-catalyzed oxidation of indole. Our results will also serve as a lighthouse in guiding the engineering of CPO into an efficient biocatalyst for synthetic and pharmaceutical applications.

ASSOCIATED CONTENT

Supporting Information

Details of the parametrization of the ferric heme for use with the GROMOS96 force field (Table S1), distances between protons of indole and the heme iron for the CPO−indole complex obtained from relaxation experiments at pH 5.0 and the corresponding distances observed in the simulation (Table S2), rmsds and rmsfs of the active site residues (Table S3), energies averaged over last 50 ps of the simulation (Table S4), distances between protons of indole and the heme iron as a function of simulation time (Figure S1), and rmsds of the active site residues during the last 50 ps of the simulation (Figure S2). This material is available free of charge via the Internet at http://pubs.acs.org.

AUTHOR INFORMATION

Corresponding Author

*E-mail: wangx@fiu.edu. Phone: (305) 348-7544.

Funding

This research is supported by the National Science Foundation via Grant CHE-0540763 to X.W. (CAREER Award), a start-up fund from Florida International University, and National Institutes of Health Grant SC3GM83723 to D.C.

Notes

The authors declare no competing financial interest.

ACKNOWLEDGMENTS

We are grateful to Florida International University's NMR facility for the use of its Bruker Avance 600 MHz spectrometer sponsored by U.S. Department of Defense Grant AR-O:W911NF0411-0022.

ABBREVIATIONS

CPO, chloroperoxidase; CPDO, 1,3-cyclopentanedione; CYP1A1, cytochrome P450, family 1, member A1; DSS, 4,4-dimethyl-4-silapentane-1-sulfonic acid; K_D, dissociation constant; MD, molecular dynamics; MP2, second-order Møller−Plesset perturbation theory; NMR, nuclear magnetic resonance; R_Z, Reinheitszahl; rmsd, root-mean-square deviation; SPC, simple point charge; T_1, longitudinal relaxation time; P450, cytochrome P450; P450 BM3, cytochrome P450 BM3; PDB, Protein Data Bank; Pca, pyroglutamic acid; PME, particle mesh Ewald method.

REFERENCES

(1) Morris, D. R., and Hager, L. P. (1966) Chloroperoxidase I. Isolation and properties of the crystalline glycoprotein. *J. Biol. Chem. 241*, 1763−1768.

(2) Sundaramoorthy, M., Terner, J., and Poulos, T. L. (1995) The crystal structure of chloroperoxidase: A heme peroxidase-cytochrome P450 functional hybrid. *Structure (Oxford, U.K.) 3*, 1367−1378.

(3) Hager, L. P., Morris, D. R., Brown, F. S., and Eberwein, H. (1966) Chloroperoxidase II. Utilization of halogen anions. *J. Biol. Chem. 241*, 1769−1777.

(4) Osborne, R. L., Raner, G. M., Hager, L. P., and Dawson, J. H. (2006) *C. fumago* chloroperoxidase is also a dehaloperoxidase: Oxidative dehalogenation of halophenols. *J. Am. Chem. Soc. 128*, 1036−1037.

(5) Kedderis, G. L., Koop, D. R., and Hollenberg, P. F. (1980) *N*-Demethylation reactions catalyzed by chloroperoxidase. *J. Biol. Chem. 255*, 10174−10182.

(6) Allain, E. J., Hager, L. P., Deng, L., and Jacobsen, E. N. (1993) Highly enantioselective epoxidation of disubstituted alkenes with hydrogen peroxide catalyzed by chloroperoxidase. *J. Am. Chem. Soc. 115*, 4415−4416.

(7) Carmichael, R., Fedorak, P. M., and Pickard, M. A. (1985) Oxidation of phenols by chloroperoxidase. *Biotechnol. Lett. 7*, 289−294.

(8) Colonna, S., Gaggero, N., Manfredi, A., Casella, L., Gullotti, M., Carrea, G., and Pasta, P. (1990) Enantioselective oxidations of sulfides catalyzed by chloroperoxidase. *Biochemistry 29*, 10465−10468.

(9) Corbett, M. D., Baden, D. G., and Chipko, B. R. (1979) Arylamine oxidations by chloroperoxidase. *Bioorg. Chem. 8*, 91−95.

(10) Geigert, J., Dalietos, D. J., Neidleman, S. L., Lee, T. D., and Wadsworth, J. (1983) Peroxide oxidation of primary alcohols to aldehydes by chloroperoxidase catalysis. *Biochem. Biophys. Res. Commun. 114*, 1104−1108.

(11) Kiljunen, E., and Kanerva, L. T. (2000) Chloroperoxidase-catalysed oxidation of alcohols to aldehydes. *J. Mol. Catal. B: Enzym. 9*, 163−172.

(12) Hager, L. P. (2010) A lifetime of playing with enzymes. *J. Biol. Chem. 285*, 14852−14860.
(13) Hager, L. P., Lakner, F. J., and Basavapathruni, A. (1998) Chiral synthons via chloroperoxidase catalysis. *J. Mol. Catal. B: Enzym. 5*, 95−101.
(14) Lakner, F. J., Cain, K. P., and Hager, L. P. (1997) Enantioselective epoxidation of ω-bromo-2-methyl-1-alkenes catalyzed by chloroperoxidase. Effect of chain length on selectivity and efficiency. *J. Am. Chem. Soc. 119*, 443−444.
(15) Lakner, F. J., and Hager, L. P. (1996) Chloroperoxidase as enantioselective epoxidation catalyst: An efficient synthesis of (R)-(−)-mevalonolactone. *J. Org. Chem. 61*, 3923−3925.
(16) Zaks, A., and Dodds, D. R. (1995) Chloroperoxidase-catalyzed asymmetric oxidations: Substrate specificity and mechanistic study. *J. Am. Chem. Soc. 117*, 10419−10424.
(17) Dawson, J. H. (1988) Probing structure-function relations in heme-containing oxygenases and peroxidases. *Science 240*, 433−439.
(18) Dawson, J. H., and Sono, M. (1987) Cytochrome P-450 and chloroperoxidase: Thiolate-ligated heme enzymes. Spectroscopic determination of their active-site structures and mechanistic implications of thiolate ligation. *Chem. Rev. 87*, 1255−1276.
(19) Woggon, W. D., Wagenknecht, H. A., and Claude, C. (2001) Synthetic active site analogues of heme-thiolate proteins: Characterization and identification of intermediates of the catalytic cycles of cytochrome P450cam and chloroperoxidase. *J. Inorg. Biochem. 83*, 289−300.
(20) Torres, E., and Ayala, M. (2010) Challenges in the application of peroxidases. In *Biocatalysis based on heme peroxidases: Peroxidases as potential industrial biocatalysts*, pp 209−352, Springer, New York.
(21) Sundaramoorthy, M., Terner, J., and Poulos, T. L. (1998) Stereochemistry of the chloroperoxidase active site: Crystallographic and molecular-modeling studies. *Chem. Biol. 5*, 461−473.
(22) Kühnel, K., Blankenfeldt, W., Terner, J., and Schlichting, I. (2006) Crystal structures of chloroperoxidase with its bound substrates and complexed with formate, acetate, and nitrate. *J. Biol. Chem. 281*, 23990−23998.
(23) Wang, X., and Goff, H. M. (1997) A nuclear paramagnetic relaxation study of the interaction of the cyclopentanedione substrate with chloroperoxidase. *Biochim. Biophys. Acta 1339*, 88−96.
(24) Bakhmutov, V. I. (2005) Paramagnetic NMR Relaxation. In *Practical nuclear magnetic resonance relaxation for chemists*, pp 179−193, Wiley, New York.
(25) Otting, G. (2010) Protein NMR using paramagnetic ions. *Annu. Rev. Biophys. 39*, 387−405.
(26) Modi, S., Primrose, W. U., Boyle, J. M. B., Gibson, C. F., Lian, L. Y., and Roberts, G. C. K. (1995) NMR studies of substrate binding to cytochrome P450 BM3: Comparisons to cytochrome P450cam. *Biochemistry 34*, 8982−8988.
(27) Solomon, I. (1955) Relaxation processes in a system of two spins. *Phys. Rev. 99*, 559.
(28) Casella, L., Gullotti, M., Selvaggini, C., Poli, S., Beringhelli, T., and Marchesini, A. (1994) The chloroperoxidase-catalyzed oxidation of phenols. Mechanism, selectivity, and characterization of enzyme-substrate complexes. *Biochemistry 33*, 6377−6386.
(29) Casella, L., Gullotti, M., Ghezzi, R., Poli, S., Beringhelli, T., Colonna, S., and Carrea, G. (1992) Mechanism of enantioselective oxygenation of sulfides catalyzed by chloroperoxidase and horseradish peroxidase. Spectral studies and characterization of enzyme-substrate complexes. *Biochemistry 31*, 9451−9459.
(30) Bikiel, D. E., Boechi, L., Capece, L., Crespo, A., De Biase, P. M., Di Lella, S., Lebrero, M. C. G., Martí, M. A., Nadra, A. D., and Perissinotti, L. L. (2006) Modeling heme proteins using atomistic simulations. *Phys. Chem. Chem. Phys. 8*, 5611−5628.
(31) van Gunsteren, W. F., Dolenc, J., and Mark, A. E. (2008) Molecular simulation as an aid to experimentalists. *Curr. Opin. Struct. Biol. 18*, 149−153.
(32) Brünger, A. T., Adams, P. D., and Rice, L. M. (1997) New applications of simulated annealing in X-ray crystallography and solution NMR. *Structure (Oxford, U.K.) 5*, 325−336.
(33) Clore, G. M., and Schwieters, C. D. (2002) Theoretical and computational advances in biomolecular NMR spectroscopy. *Curr. Opin. Struct. Biol. 12*, 146−153.
(34) Roberts, A. G., Sjögren, S. E. A., Fomina, N., Vu, K. T., Almutairi, A., and Halpert, J. R. (2011) NMR-derived models of amidopyrine and its metabolites complexed to rabbit cytochrome P450 2B4 reveal a structural mechanism of sequential *N*-dealkylation. *Biochemistry 50*, 2123−2134.
(35) Roberts, A. G., Yang, J., Halpert, J. R., Nelson, S. D., Thummel, K. T., and Atkins, W. M. (2011) The structural basis for homotropic and heterotropic cooperativity of midazolam metabolism by human cytochrome P450 3A4. *Biochemistry 50*, 10804−10818.
(36) Corbett, M. D., and Chipko, B. R. (1979) Peroxide oxidation of indole to oxindole by chloroperoxidase catalysis. *Biochem. J. 183*, 269−276.
(37) van Deurzen, M. P. J., van Rantwijk, F., and Sheldon, R. A. (1996) Synthesis of substituted oxindoles by chloroperoxidase catalyzed oxidation of indoles. *J. Mol. Catal. B: Enzym. 2*, 33−42.
(38) Hallenberg, P. F., and Hager, L. P. (1978) Purification of chloroperoxidase from *Caldariomyces fumago*. *Methods Enzymol. 52*, 521−529.
(39) Hashimoto, A., and Pickard, M. A. (1984) Chloroperoxidases from *caldariomyces* (= *leptoxyphium*) cultures: Glycoproteins with variable carbohydrate content and isoenzymic forms. *J. Gen. Microbiol. 130*, 2051−2058.
(40) Vold, R. L., Waugh, J. S., Klein, M. P., and Phelps, D. E. (1968) Measurement of spin relaxation in complex systems. *J. Chem. Phys. 48*, 3831−3832.
(41) Rea, V., Kolkman, A. J., Vottero, E., Stronks, E. J., Ampt, K. A. M., Honing, M., Vermeulen, N. P. E., Wijmenga, S. S., and Commandeur, J. N. M. (2012) Active site substitution A82W improves the regioselectivity of steroid hydroxylation by cytochrome P450 BM3 mutants as rationalized by spin relaxation nuclear magnetic resonance studies. *Biochemistry 51*, 750−760.
(42) Sakurada, J., Takahashi, S., and Hosoya, T. (1986) Nuclear magnetic resonance studies on the spatial relationship of aromatic donor molecules to the heme iron of horseradish peroxidase. *J. Biol. Chem. 261*, 9657−9662.
(43) Cameron, M. D., Wen, B., Allen, K. E., Roberts, A. G., Schuman, J. T., Campbell, A. P., Kunze, K. L., and Nelson, S. D. (2005) Cooperative binding of midazolam with testosterone and α-naphthoflavone within the CYP3A4 active site: A NMR T_1 paramagnetic relaxation study. *Biochemistry 44*, 14143−14151.
(44) Morris, G. M., Goodsell, D. S., Halliday, R. S., Huey, R., Hart, W. E., Belew, R. K., and Olson, A. J. (1998) Automated docking using a Lamarckian genetic algorithm and an empirical binding free energy function. *J. Comput. Chem. 19*, 1639−1662.
(45) Oostenbrink, C., Villa, A., Mark, A. E., and Van Gunsteren, W. F. (2004) A biomolecular force field based on the free enthalpy of hydration and solvation: The GROMOS force-field parameter sets 53A5 and 53A6. *J. Comput. Chem. 25*, 1656−1676.
(46) Zong, Q., Osmulski, P. A., and Hager, L. P. (1995) High-pressure-assisted reconstitution of recombinant chloroperoxidase. *Biochemistry 34*, 12420−12425.
(47) Pickard, M. A. (1981) A defined growth medium for the production of chloroperoxidase by *Caldariomyces fumago*. *Can. J. Microbiol. 27*, 1298−1305.
(48) Neese, F. (2012) The ORCA program system. *Wiley Interdiscip. Rev.: Comput. Mol. Sci. 2*, 73−78.
(49) Head-Gordon, M., Pople, J. A., and Frisch, M. J. (1988) MP2 energy evaluation by direct methods. *Chem. Phys. Lett. 153*, 503−506.
(50) Weigend, F., and Ahlrichs, R. (2005) Balanced basis sets of split valence, triple ζ valence and quadruple ζ valence quality for H to Rn: Design and assessment of accuracy. *Phys. Chem. Chem. Phys. 7*, 3297−3305.
(51) Sanner, M. F. (1999) Python: A programming language for software integration and development. *J. Mol. Graphics Modell. 17*, 57−61.

(52) Hess, B., Kutzner, C., van der Spoel, D., and Lindahl, E. (2008) GROMACS 4: Algorithms for highly efficient, load-balanced, and scalable molecular simulation. *J. Chem. Theory Comput. 4*, 435−447.
(53) Schuttelkopf, A. W., and van Aalten, D. M. F. (2004) PRODRG: A tool for high-throughput crystallography of protein-ligand complexes. *Acta Crystallogr. D60*, 1355−1363.
(54) Lemkul, J. A., Allen, W. J., and Bevan, D. R. (2010) Practical considerations for building GROMOS-compatible small-molecule topologies. *J. Chem. Inf. Model. 50*, 2221−2235.
(55) Seminario, J. M. (1996) Calculation of intramolecular force fields from second-derivative tensors. *Int. J. Quantum Chem. 60*, 1271−1277.
(56) Breneman, C. M., and Wiberg, K. B. (1990) Determining atom-centered monopoles from molecular electrostatic potentials. The need for high sampling density in formamide conformational analysis. *J. Comput. Chem.*, 361−373.
(57) Berendsen, H. J. C., Postma, J. P. M., van Gunstetren, W. F., and Hermans, J. (1981) Interaction models for water in relation to protein hydration. In *Intermolecular forces*, pp 331−342, D. Reidel Publishing Co., Dordrecht, The Netherlands.
(58) Darden, T., York, D., and Pedersen, L. (1993) Particle mesh Ewald: An N·log(N) method for Ewald sums in large systems. *J. Chem. Phys. 98*, 10089−10092.
(59) Hess, B., Bekker, H., Berendsen, H. J. C., and Fraaije, J. G. E. M. (1997) LINCS: A linear constraint solver for molecular simulations. *J. Comput. Chem. 18*, 1463−1472.
(60) van Deurzen, M. P. J., Remkes, I. J., Van Rantwijk, F., and Sheldon, R. A. (1997) Chloroperoxidase catalyzed oxidations in *t*-butyl alcohol/water mixtures. *J. Mol. Catal. A: Chem. 117*, 329−337.
(61) Huang, W. C., Westlake, A. C., Maréchal, J. D., Joyce, M. G., Moody, P. C., and Roberts, G. C. (2007) Filling a hole in cytochrome P450 BM3 improves substrate binding and catalytic efficiency. *J. Mol. Biol. 373*, 633−651.
(62) Constantine, K. L. (2001) Evaluation of site-directed spin labeling for characterizing protein-ligand complexes using simulated restraints. *Biophys. J. 81*, 1275−1284.
(63) Yue, S. Y. (1990) Distance-constrained molecular docking by simulated annealing. *Protein Eng. 4*, 177−184.
(64) Pickard, M. A., Kadima, T. A., and Carmichael, R. D. (1991) Chloroperoxidase, a peroxidase with potential. *J. Ind. Microbiol. Biotechnol. 7*, 235−241.
(65) Manoj, K. M., and Hager, L. P. (2001) Utilization of peroxide and its relevance in oxygen insertion reactions catalyzed by chloroperoxidase. *Biochim. Biophys. Acta 1547*, 408−417.
(66) Hinman, R. L., and Whipple, E. B. (1962) The protonation of indoles: Position of protonation. *J. Am. Chem. Soc. 84*, 2534−2539.
(67) Butler, A., and Sandy, M. (2009) Mechanistic considerations of halogenating enzymes. *Nature 460*, 848−854.
(68) Vaillancourt, F. H., Yeh, E., Vosburg, D. A., Garneau-Tsodikova, S., and Walsh, C. T. (2006) Nature's inventory of halogenation catalysts: Oxidative strategies predominate. *Chem. Rev. 106*, 3364−3378.
(69) Filizola, M., and Loew, G. H. (2000) Probing the role of protein environment in compound I formation of chloroperoxidase (CPO). *J. Am. Chem. Soc. 122*, 3599−3605.
(70) Yi, X., Conesa, A., Punt, P. J., and Hager, L. P. (2003) Examining the role of glutamic acid 183 in chloroperoxidase catalysis. *J. Biol. Chem. 278*, 13855−13859.
(71) Morozov, A. N., and Chatfield, D. C. (2012) Chloroperoxidase-catalyzed epoxidation of *cis*-*β*-methylstyrene: Distal pocket flexibility tunes catalytic reactivity. *J. Phys. Chem. B 116*, 12905−12914.
(72) Baciocchi, E., Fabbrini, M., Lanzalunga, O., Manduchi, L., and Pochetti, G. (2001) Prochiral selectivity in H_2O_2-promoted oxidation of arylalkanols catalysed by chloroperoxidase. *Eur. J. Biochem. 268*, 665−672.
(73) Huey, R., Morris, G. M., Olson, A. J., and Goodsell, D. S. (2007) A semiempirical free energy force field with charge-based desolvation. *J. Comput. Chem. 28*, 1145−1152.
(74) Li, W., Tang, Y., Hoshino, T., and Neya, S. (2009) Molecular modeling of human cytochrome P450 2W1 and its interactions with substrates. *J. Mol. Graphics Modell. 28*, 170−176.
(75) Gay, S. C., Roberts, A. G., Maekawa, K., Talakad, J. C., Hong, W. X., Zhang, Q., Stout, C. D., and Halpert, J. R. (2010) Structures of cytochrome P450 2B4 complexed with the antiplatelet drugs ticlopidine and clopidogrel. *Biochemistry 49*, 8709−8720.
(76) Huang, Q., Deshmukh, R. S., Ericksen, S. S., Tu, Y., and Szklarz, G. D. (2012) Preferred binding orientations of phenacetin in CYP 1A1 and 1A2 are associated with isoform-selective metabolism. *Drug Metab. Dispos. 40*, 2324−2331.
(77) Chen, H., Hirao, H., Derat, E., Schlichting, I., and Shaik, S. (2008) Quantum mechanical/molecular mechanical study on the mechanisms of compound I formation in the catalytic cycle of chloroperoxidase: An overview on heme enzymes. *J. Phys. Chem. B 112*, 9490−9500.
(78) Wang, X., Tachikawa, H., Yi, X., Manoj, K. M., and Hager, L. P. (2003) Two-dimensional NMR study of the heme active site structure of chloroperoxidase. *J. Biol. Chem. 278*, 7765−7774.
(79) Manoj, K. M., and Hager, L. P. (2008) Chloroperoxidase, a Janus Enzyme? *Biochemistry 47*, 2997−3003.
(80) Morozov, A. N., D'Cunha, C., Alvarez, C. A., and Chatfield, D. C. (2011) Enantiospecificity of chloroperoxidase-catalyzed epoxidation: Biased molecular dynamics study of a *cis*-*β*-methylstyrene/chloroperoxidase-compound I complex. *Biophys. J. 100*, 1066−1075.
(81) Aburto, J., Correa-Basurto, J., and Torres, E. (2008) Atypical kinetic behavior of chloroperoxidase-mediated oxidative halogenation of polycyclic aromatic hydrocarbons. *Arch. Biochem. Biophys. 480*, 33−40.
(82) Stone, K. L., Behan, R. K., and Green, M. T. (2005) X-ray absorption spectroscopy of chloroperoxidase compound I: Insight into the reactive intermediate of P450 chemistry. *Proc. Natl. Acad. Sci. U.S.A. 102*, 16563−16565.
(83) Kuhnel, K., Derat, E., Terner, J., Shaik, S., and Schlichting, I. (2007) Structure and quantum chemical characterization of chloroperoxidase compound 0, a common reaction intermediate of diverse heme enzymes. *Proc. Natl. Acad. Sci. U.S.A. 104*, 99−104.
(84) Porro, C. S., Sutcliffe, M. J., and de Visser, S. P. (2009) Quantum mechanics/molecular mechanics studies on the sulfoxidation of dimethyl sulfide by compound I and compound 0 of cytochrome P450: Which is the better oxidant? *J. Phys. Chem. A 113*, 11635−11642.
(85) Rutter, R., Hager, L. P., Dhonau, H., Hendrich, M., Valentine, M., and Debrunner, P. (1984) Chloroperoxidase compound I: Electron paramagnetic resonance and Mössbauer studies. *Biochemistry 23*, 6809−6816.
(86) Kim, S. H., Perera, R., Hager, L. P., Dawson, J. H., and Hoffman, B. M. (2006) Rapid freeze-quench ENDOR study of chloroperoxidase compound I: The site of the radical. *J. Am. Chem. Soc. 128*, 5598−5599.
(87) Green, M. T., Dawson, J. H., and Gray, H. B. (2004) Oxoiron(IV) in chloroperoxidase compound II is basic: Implications for P450 chemistry. *Science 304*, 1653−1656.
(88) Cooper, H. L. R., and Groves, J. T. (2011) Molecular probes of the mechanism of cytochrome P450. Oxygen traps a substrate radical intermediate. *Arch. Biochem. Biophys. 507*, 111−118.
(89) Tuynman, A., Vink, M. K. S., Dekker, H. L., Schoemaker, H. E., and Wever, R. (2001) The sulphoxidation of thioanisole catalysed by lactoperoxidase and *Coprinus cinereus* peroxidase: Evidence for an oxygen-rebound mechanism. *Eur. J. Biochem. 258*, 906−913.
(90) Gross, Z., and Nimri, S. (1995) Seeing the long-sought intermediate in the reaction of oxoiron(IV) porphyrin cation radicals with olefins. *J. Am. Chem. Soc. 117*, 8021−8022.
(91) Takahashi, A., Kurahashi, T., and Fujii, H. (2011) Redox potentials of oxoiron(IV) porphyrin *π*-cation radical complexes: Participation of electron transfer process in oxygenation reactions. *Inorg. Chem. 50*, 6922−6928.
(92) Bukowski, M. R., Koehntop, K. D., Stubna, A., Bominaar, E. L., Halfen, J. A., Münck, E., Nam, W., and Que, L., Jr. (2005) A thiolate-

ligated nonheme oxoiron(IV) complex relevant to cytochrome P450. *Science 310*, 1000−1002.
(93) Green, M. T. (2009) CH bond activation in heme proteins: The role of thiolate ligation in cytochrome P450. *Curr. Opin. Chem. Biol. 13*, 84−88.
(94) Osborne, R. L., Coggins, M. K., Terner, J., and Dawson, J. H. (2007) *Caldariomyces fumago* chloroperoxidase catalyzes the oxidative dehalogenation of chlorophenols by a mechanism involving two one-electron steps. *J. Am. Chem. Soc. 129*, 14838−14839.